Calcium-dependent cytosolic phospholipase A2 activation is implicated in neuroinflammation and oxidative stress associated with ApoE4

Shaowei Wang
   USC: University of Southern California

Boyang Li
   University of Southern California

Victoria Solomon
   University of Southern California

Alfred Fonteh
   Huntington Medical Research Institutes

Stanley I. Rapoport
   NIAAA: National Institute on Alcohol Abuse and Alcoholism

David A. Bennett
   Rush University Medical Center

Zoe Arvanitakis
   Rush University Medical Center

Helena C. Chui
   USC: University of Southern California

Carol A. Miller
   USC: University of Southern California

Patrick M. Sullivan
   Duke University

Hussein Yassine
   University of Southern California

Research article

Keywords: cPLA2, ApoE4, Alzheimer's disease, p38, Oxidative stress

---

Abstract

Background

Apolipoprotein E4 (*APOE4*) is associated with a greater response to neuroinflammation and risk of developing late-onset Alzheimer disease (AD), but the mechanisms for this association are not clear. Activation of calcium-dependent cytosolic phospholipase A2 (cPLA2) is involved in inflammatory signaling and is elevated within plaques of the AD brain. The relation between *APOE4* genotype and cPLA2 activity is not known.

Methods

Mouse primary astrocytes, mouse and human brain samples differing by *APOE* genotypes were collected for measuring cPLA2 expression, phosphorylation and activity in relation to measures of inflammation and oxidative stress.

Results

Greater cPLA2 phosphorylation and activity were identified in ApoE4 compared to ApoE3 in primary astrocytes and brains of ApoE-targeted replacement (ApoE-TR) mice. These differences were also demonstrated in brain homogenates from the inferior frontal cortex from AD patients carrying *APOE3/4* compared to *APOE3/3*. Higher cPLA2 activation with *APOE4* was associated with greater activation of the MAPK p38 pathway, as well as with higher levels of leukotriene B4 (LTB4), reactive oxygen species (ROS) and inducible nitric oxide synthase (iNOS). Inhibition of cPLA2 reduced LTB4, ROS and iNOS levels in ApoE4 primary astrocytes to those of ApoE3 astrocytes.

Conclusions

Our findings implicate greater activation of cPLA2 signaling system with *APOE4*, that could represent a potential drug target for mitigating the increased neuroinflammation with *APOE4* and AD.

Background

The enzyme phospholipase A2 (PLA2) catalyzes the hydrolysis of the stereo-specifically numbered (sn-2) ester bond of substrate phospholipids in the cell membrane, to produce a free fatty acid and a lyso-phospholipid [1]. Calcium-independent PLA2 (iPLA2) has a greater affinity for releasing docosahexaenoic acid (DHA, 22:6 n-3), which acts as a signaling molecule during neurotransmission and as a precursor of anti-inflammatory and antioxidant resolvins [2, 3]. Calcium-dependent cytosolic phospholipase A2 (cPLA2) releases arachidonic acid (AA, 20:4 n-6), which plays important functions in storing energy, as a second messenger in neurotransmission, and as a the precursor of eicosanoids [4, 5]. Free AA can be

oxidized by cyclooxygenase (COX) or lipoxygenase (LOX) to produce prostaglandins or leukotrienes, which are potent mediators of inflammation [1, 6]. In astrocytes, cPLA2 interacts with mitochondrial antiviral-signaling protein (MAVS) to boost nuclear factor kappa-light-chain-enhancer of activated B cells (NF-kB)-driven inflammatory responses [7]. In microglia, cPLA2 and AA metabolic pathways contribute to reactive oxygen species (ROS) and nitric oxide (NO) production during cell activation[8]. cPLA2 activity depends on its phosphorylation, which is regulated by mitogen-activated protein kinase (MAPK) pathways [9, 10].

A lower amount of Aβ oligomers and the absence of markers of glial activation in both astrocytic and microglia distinguish the brains of individuals with greater brain Aβ plaques and tangles but resilience to AD dementia from those with dementia [11]. cPLA2 activation is one of the pathways that activates microglia and astrocytes in the brain. The cPLA2 gene, protein levels, and its phosphorylated form are increased around plaques of AD brains compared to healthy controls [12–14]. In AD animal models, increased activation of cPLA2 is observed in the hippocampus of human amyloid precursor protein (hAPP) transgenic mice [14]. The activation of cPLA2 by Aβ oligomers is believed to contribute to a dysregulation of fatty acid metabolism, promoting neurodegeneration [15, 16]. Overexpression of p25 in neurons increases the expression of cPLA2 leading to lysophosphatidylcholine (LPC) secretion, and to the activation of astrocytes and production of pro-inflammatory cytokines [17]. Conversely, cPLA2 deficiency in AD mouse models ameliorates the memory impairment and hyperactivated glial cells observed in AD mouse models [14, 18]. Knocking out cPLA2 in microglia decreases lipopolysaccharide (LPS) induced oxidative stress and inflammatory response [8].

Carrying the *APOE4* allele is the strongest genetic risk factor for late-onset AD. The ApoE4 protein seems to have proinflammatory and/or reduced anti-inflammatory functions, which could exacerbate AD pathology. This was clearly demonstrated in the Framingham cohort where participants with *APOE4* and elevated plasma C-reactive protein (CRP) levels had a greater risk of developing late-onset of AD than age and sex-matched *APOE2* and *APOE3* carriers [19]. In brains of participants with AD, *APOE4* is associated with greater levels of lipid peroxidation, eicosanoids and oxidative stresses markers [20], but the mechanisms for these observations are not clear. Here, we hypothesized that ApoE4 activates cPLA2 to enhance AA release and eicosanoid levels, leading to an enhanced inflammatory and oxidative stress response. Accordingly, we examined cPLA2 expression and activation in mouse primary astrocytes, mouse and human brain samples that differed by *APOE* genotype and determined the cellular effects of cPLA2 inhibition on measurements of neuroinflammation and oxidative stress.

Results

1. cPLA2 and phosphorylated cPLA2 are increased in ApoE4 mouse primary astrocytes

We previously found that DHA/AA ratio in cerebrospinal fluid (CSF) is lower in *APOE4/E4* carriers compared to *APOE3/E3* carriers [21, 22]. Since astrocytic cPLA2 and iPLA2 enzymes are important determinants of brain AA and DHA metabolism [2, 23], the expression and activity of these enzymes were

examined in primary astrocytes from ApoE-TR mice. ApoE4 astrocytes had greater mRNA and protein levels of cPLA2 and phosphorylated cPLA2 compared with ApoE3 astrocytes (Fig. 1A, B). In contrast, iPLA2 mRNA and protein levels did not differ between ApoE4 and ApoE3 primary astrocytes (Fig.1C, D). These measures were also significantly greater in ApoE4 immortalized astrocytes compared to ApoE3 (Fig. S1). To further explore the activity of cPLA2 and iPLA2, the efflux of ^{3}H-AA or ^{14}C-DHA from ApoE3 and ApoE4 primary astrocyte cells to media with or without ATP stimulation for 15 min was examined. ^{3}H-AA efflux was significantly greater in stimulated ApoE4 compared to ApoE3 primary astrocytes (Fig. 1E), whereas ^{14}C-DHA efflux showed no difference between ApoE4 and ApoE3 (Fig. 1F). To confirm the effect of the ApoE protein, cultured primary astrocytes from C57BL/6 mice were labeled with ^{3}H-AA or ^{14}C-DHA and then treated with 0.2 μM rApoE3 or rApoE4 proteins for 24h under similar conditions to primary astrocytes cultured from ApoE-TR mice. ^{3}H-AA efflux was greater after rApoE4 than rApoE3 treatment (Fig. 1G), whereas DHA efflux did not differ between rApoE4 and rApoE3 treatments (Fig. 1H). Taken together, these results confirmed that cPLA2 expression and activity were greater in ApoE4 compared to ApoE3 astrocytes.

2. Phosphorylated cPLA2 and cPLA2 activity are increased in *APOE4* mouse brains

To investigate the effect of the ApoE isoforms on cPLA2 *in vivo*, mRNA, total protein, and phosphorylated protein levels of cPLA2 were measured in the cerebral cortex from 8-month-old of ApoE3-TR and ApoE4-TR mice. There was no difference in cortical cPLA2 mRNA levels between ApoE3-TR and ApoE4-TR mice (Fig. 2A). Since phosphorylated cPLA2 levels were too low to detect in total brain homogenates, cPLA2 was enriched by immunoprecipitation with a cPLA2 antibody using 500 μg of cortical homogenate, and total and phosphorylated cPLA2 were measured by immunoblotting. Total cPLA2 levels did not differ between ApoE3-TR and ApoE4-TR mouse cortex (Fig. 2B). However, phosphorylated cPLA2 was significantly increased in ApoE4-TR mouse cortex compared to ApoE3-TR mouse cortex (Fig. 2B). Consistent with these observations, cortical cPLA2 activity was greater in ApoE4-TR than ApoE3-TR mice (Fig. 2C).

1. p38 MAPK but not ERK1/2 is increased in ApoE4 mouse primary astrocytes

Phosphorylation of cPLA2 is regulated by MAPK pathways, including p38 MAPK and ERK1/2 MAPK [10, 24, 25]. We tested the phosphorylation of p38 and ERK1/2 in primary astrocytes and in mouse cortex from ApoE3 or ApoE4-TR mice by immunoblot using antibodies against total and phosphorylated proteins. Total p38 and ERK1/2 proteins did not differ between ApoE3 and ApoE4 primary astrocytes (Fig. 3A). Interestingly, only phosphorylated p38, but not phosphorylated ERK1/2, was significantly greater in ApoE4 primary astrocyte compared with ApoE3 primary astrocytes (Fig. 3A). This finding suggests that the greater phosphorylation of cPLA2 observed in ApoE4 is driven by p38 MAPK activation, but not the ERK1/2 MAPK pathway. In agreement, greater p38 phosphorylation but not of ERK1/2 was evident in the cerebral cortex of 8-months old ApoE4-TR mice compared to ApoE3-TR mice (Fig. 3B).

2. phosphorylated cPLA2 is increased in *APOE4* human brains

Table 1 Characteristics of clinical samples

Regions sampled and source	Inferior frontal lobe (ROSMAP, RUSH ADRC)				Hippocampus, USC ADRC	
Clinical diagnosis	AD	AD	NCI	NCI	NCI	AD
Genotype	E3/E3	E3/E4	E3/E3	E3/E4	E3/E3	E4/E4
Sample size, n	12	10	12	10	7	9
Age (years ± SD) *	92±6	95±5	83±5	85±4	85±5	78±6
Sex (n, female/male) *	5/7	6/4	6/6	5/5	5/2	6/3
Braak stage	IV	V	III	III	I	V

 *Age and gender did not differ between groups compared using ANOVA. NCI=no cognitive impairment. AD=Alzheimer's disease.

To determine where these findings can be demonstrated in human brains, we first compared the total and phosphorylated forms of cPLA2 in human hippocampus samples from individuals with no cognitive impairment (NCI) and homozygous *APOE3 (APOE3/E3)* carriers with individuals with AD and homozygous *APOE4 (APOE4/E4)*. Characteristics of brain samples tested are summarized in Table 1. After enrichment of cPLA2 protein, phosphorylated and total protein levels of cPLA2 were detected by Western Blot. There was no difference in total cPLA2 protein between *APOE3/E3* and *APOE4/E4* human hippocampus, while phosphorylated cPLA2 trended toward an increase in *APOE4/E4* human hippocampus compared to that of *APOE3/E3* carriers. However, this difference did not reach statistical significance, likely a result of the small size of samples of the human brain samples (Fig. 4A). Moreover, this comparison was limited by virtue of a comparison that included both disease state and *APOE* genotype. To overcome this limitation, we compared phosphorylated and total cPLA2 in the inferior frontal cortex of persons with similar clinical diagnosis but with different *APOE* genotypes. After a similar enrichment of cPLA2 from the cortex, phosphorylated and total cPLA2 were measured by Western Blot. In the NCI group, total cPLA2 did not significantly differ between the *APOE3/E3* and *APOE3/E4* carriers, while the phosphorylated cPLA2 level showed a trend increase in *APOE3/E4* carriers compared to *APOE3/E3* carriers (Fig. 4B). In patients with AD, phosphorylated cPLA2 levels were significantly greater in *APOE3/*E4 carriers compared with *APOE3/E3* carriers (p=0.039), while the total cPLA2 levels did not differ between the two groups (Fig. 4C). Greater cPLA2 phosphorylation in *APOE3/4* group was not affected by sex, age or Braak stage.

3. p38 MAPK is increased in *APOE4* human brain samples

Previous results from mouse astrocyte and cortex showed increased p38 activation in ApoE4-TR compared to ApoE3-TR mice. In agreement, greater levels of phosphorylated p38 in the hippocampus of the *APOE4/E4* AD group were observed compared to the *APOE3/E3* NCI group (Fig. 5A). Phosphorylated

and total p38 levels did not differ between NCI *APOE3/E3* and NCI *APOE3/E4* groups (Fig. 5B), while total p38 level was significantly greater in the AD *APOE3/E4* group compared with the AD *APOE3/E3* group (Fig. 5C). These results support that the greater activation of cPLA2 in ApoE4 might be regulated by the p38 MAPK pathway and is most prominent in persons with AD.

4. LTB4 levels is increased in *APOE4* human brain samples

AA is released by cPLA2 hydrolysis of membrane phospholipids, which then can be rapidly oxidized by COX or LOX enzymes to prostaglandins or leukotrienes (LTB4 and PGE2), potent mediators of inflammation and signal transduction [2]. To test the effect of the greater cPLA2 phosphorylation in *APOE4* AD brains, PGE2 and LTB4 levels were assayed in the brain homogenates from the inferior frontal cortex. LTB4 levels were significantly greater in the AD *APOE3/4* group compared with the AD *APOE3/3* group (p=0.01) (Fig. 6A), while PGE2 levels did not differ between the two groups (Fig. 6B). The greater LTB4 levels in APOE3/E4 group were also not affected by sex, age or Braak stage. No significant differences were found in either LTB4 or PGE2 levels between the NCI *APOE3/4* and NCI *APOE3/4* groups (Fig. 6C and D). The expression of 5-LOX and COX-2 did not differ between the AD *APOE3/3* and AD *APOE3/4* groups (Fig. 6E). These results indicate that ApoE4's activation of cPLA2 in AD selectively increases LTB4 levels in the AD brain.

5. The NF-kB inflammasome is not induced in the *APOE4* brain

It is not clear whether *APOE4* can induce neuroinflammation via activation of the NF-kB inflammasome *in vivo*, and whether cPLA2 is involved in this pathway. Although we found greater TNFa mRNA levels in ApoE4 than in ApoE3 astrocytes, IL1b, IL6 and Ccl2 did not differ between ApoE3 and ApoE4 astrocytes (Fig. 7A). In addition, none of these cytokines and chemokines differed by genotype among the mouse brain (Fig. 7B) or the human brain samples (Fig. 7D), including glial fibrillary acid protein (GFAP) for astrocytes and ionized calcium binding adaptor molecule 1 (Iba1) for microglia (Fig. 7D-E). These results indicate that neuroinflammation with *APOE4* does not favor the NF-kB inflammatory response pathway.

6. cPLA2 is involved in the ApoE4 mediated up-regulation of LTB4 and ROS

To explore whether inhibition of cPLA2 mitigates the downstream effects of LTB4 production on ROS and iNOS, ApoE3 and ApoE4 primary astrocytes were treated with the cPLA2 inhibitor pyrrophenone (Fig 8A). Treatment with pyrrophenone reduced LTB4 levels in both ApoE3 and ApoE4 astrocytes, but to a greater extent with ApoE4 astrocytes (Fig. 8B). Furthermore, cPLA2 inhibition significantly decreased ROS and iNOS expression in both ApoE3 and ApoE4 primary astrocytes (Fig. 8C). These results indicated that greater cPLA2 activity is also involved in mediating the greater levels of iNOS and ROS in the ApoE4 group and can be reduced with cPLA2 inhibition.

Discussion

Despite multiple past observations associating *APOE4* with greater neuroinflammatory and oxidative stress response than *APOE2* or *APOE3* (Table 2), the underlying mechanisms are not clearly understood. Here, we identify a plausible mechanism where *APOE4* induces greater activation of the MAPK p38-cPLA2 system, leading to greater release of AA, LTB4, iNOS and generation of ROS in astrocytes. The increase in LTB4 in *APOE4* was corroborated in human brain samples matched by disease state. Inhibition of cPLA2 activity lowered the greater measurements of neuroinflammation associated with *APOE4*, reinforcing the candidacy of cPLA2 as a therapeutic target for mitigating the increase in AD risk conferred by carrying *APOE4*.

Table 2
Summary of the association of *APOE4* with greater neuroinflammation.

Author	Key findings
Cultures (microglia, astrocytes or mixed cultures) and inflammatory response by genotype	
Vitek et al. [26]	Microglia derived from ApoE4-TR mice demonstrate increased NO production, increased NOS2 mRNA levels, and greater TNFα, IL-6, IL12 levels compared to microglia from ApoE3-TR mice.
Colton et al. [27]	Significantly more NO was produced in primary microglia and macrophages from ApoE4-TR mice compared to ApoE3-TR mice.
Guo et al [28]	Addition of exogenous ApoE4 induced greater IL1β than apoE3 in rat mixed glial cells.
Chen et al [29]	ApoE4, but not ApoE3, stimulated secretion of PGE2 and IL-1β in rat primary microglia.
Shi et al [30]	Higher TNFα, IL1β and IL1α levels were observed in primary microglia from ApoE4-TR mice stimulated with LPS than ApoE2 and ApoE3.
Tai et al [31]	Greater astrogliosis and microgliosis, higher levels of IL1β in E4FAD mice compared with E3FAD and E2FAD mice.
Zhu et al [32]	Higher levels of microglia/macrophage, astrocytes, and invading T-cells after LPS injection in ApoE4-TR mice than ApoE3-TR mice. ApoE4-TR mice also displayed greater and more prolonged increases of cytokines (IL1β, IL6, TNFα) than ApoE2 and ApoE3-TR mice.
Ophir et al [33]	The expression of inflammation-related genes (NF-κB response elements) following intracerebroventricular injection of LPS was significantly higher and more prolonged in ApoE4 than in ApoE3-TR mice.
Both human and mouse models	
Gale et al [34]	ApoE4-TR mice displayed enhanced plasma cytokines after systemic LPS compared with ApoE3 counterparts. After intravenous LPS, *APOE3/4* patients had higher plasma TNF-α levels than *APOE3/3* patients.
Human brain studies of inflammation and oxidative stress studies by APOE genotype	
Montine at al [35]	Pyramidal neuron cytoplasm was immunoreactive for 4-hydroxy-2-nonenal (HNE) in 4 of 4 *APOE4* homozygotes, 2 of 3 *APOE3/4* heterozygotes, and none of 3 *APOE3* homozygotes
Ramassamy et al al. [20]	In hippocampal homogenates from AD brains, *APOE4* carriers had greater levels of thiobarbituric acid-reactive substances (TBARS), lower activities of catalase, glutathione peroxidase and glutathione than tissues from patients homozygous for the *APOE3* allele (n = 10 per group).
Egensperger et al [36]	The number of activated microglia and the tissue area occupied by these cells increased significantly with *APOE4* gene dose (n = 20).
Minett et al [37]	*APOE4* allele was significantly related to greater expression of CD68, HLA-DR and CD64 in microglia (n = 299).

Author	Key findings
Friedberg et al [38]	Cellular density of microglial marker-Iba1 was positively associated with tau pathology in *APOE4* carrier participants only (n = 154).
Systemic inflammation and dementia risk by genotype	
Tao et al [19]	Participants with *APOE4* and elevated plasma C reactive protein (CRP) levels had a shortened latency for onset of AD (n = 2562).

There is evidence from clinical studies implicating greater cPLA2 activation around AD brain plaques [12]. cPLA2 activity is also increased in the CSF of patients with AD [39]. cPLA2 activation can be indirectly assessed by the release of AA from membrane phospholipids [2]. ^{11}C AA brain uptake by PET and AA/DHA measurement in CSF are surrogate markers of brain cPLA2 activity. Indeed, greater incorporation coefficients of ^{11}C AA by PET scans was observed in the grey-matter region of the brain of AD patients compared to control subjects [40]. Moreover, a greater AA/DHA ratio in both CSF and plasma was present in *APOE4* carriers with mild AD compared to *APOE3* carriers after DHA supplementation [21]. A greater AA/DHA ratio in plasma phospholipids in cognitively healthy *APOE4* carriers was associated with greater conversion to MCI/AD [41]. The greater plasma AA/DHA in *APOE4* suggests a systemic (for example in the liver, adipose tissues) activation of cPLA2 that is not just confined to the brain.

Greater cPLA2 activation is mechanistically involved in AD pathology and may represent one pathophysiological link between Aβ oligomers and neuroinflammatory responses [42]. An increase of phosphorylated cPLA2 but not of total cPLA2 was observed in the brains of AD mouse models compared with WT mice [14]. In *vitro* studies suggested that Aβ oligomers can trigger cPLA2 activation and PGE2 production in neurons eventually leading to neurodegeneration [43, 44]. Inhibition of cPLA2 prevented synaptic loss and memory deficits induced by Aβ oligomers in mice [45]. Similar to Aβ, there is evidence that human prion peptide can also induce neurotoxicity by activating cPLA2, which can be prevented by cPLA2 inhibition [46]. In support of greater cPLA2 activity, hippocampal levels of AA and AA-derived metabolites were much greater in hAPP mice than in non-transgenic control mice [47].

The pattern of enhanced neuroinflammation of the *APOE4* AD brains observed in this study does not support the induction of the NF-κB inflammasome (such as TNFα, IL1β, IL6 and Ccl2), as past findings supporting this activation pattern were mostly a result of high doses LPS injections in cell culture and *in vivo* animal models (summarized in Table 2). Instead, we found greater level of leukotrienes (LTB4) in the cerebral cortex of AD with E3/E4 carriers compared to E3/E3 carriers, and in apoE4 astrocytes that was associated with the greater phosphorylation of cPLA2. These observations provide a mechanism for the greater levels of oxidative stress in the *APOE4* brain [20, 35]. It is plausible that not just astrocytes, but microglia as well contribute to the greater LTB4, ROS and iNOS production with *APOE4*. A large recent proteomic and lipidomic investigation in animal brains of ApoE-TR mice corroborate the enhanced eicosanoid signaling with *APOE4* [48]. LTB4 signaling may have a prominent role in inducing oxidative stress. Chuang et al reported that ROS and NO production during microglia activation is reduced by

inhibition of lipoxygenase but not cyclooxygenase [8], suggesting induced LOX signaling as the primary driver of oxidative stress.

Activation of cPLA2 may differ by cell type and within cellular compartments. Recently, astrocytic activation of cPLA2 bound directly with MAVS enhanced NF-κB pathways to produce pro-inflammatory factors such as Ccl2 and Nos2 in an animal model of multiple sclerosis (MS) [7]. Here, we did not observe greater CcL2 or Nos2 expression in *APOE4* astrocytes, mouse or human brains suggesting that a different localization of cPLA2 activation within the astrocyte can lead to a distinct neuroinflammatory phenotype. In addition to MS, the increase in AA release and its metabolisms to prostaglandins and leukotrienes, have been observed in cancers and other neurodegeneration diseases [49–51]. For example, *PIK3CA* mutant breast cancer tumors cells displayed dramatically elevated AA and eicosanoid levels, promoting tumor cells proliferation [50].

Activation of cPLA2 activity is associated with its phosphorylation [10]. cPLA2 phosphorylation is regulated by ERKs and p38 MAPK pathways, which phosphorylates cPLA2 at Ser-505 and increases its enzymatic activity [9]. cPLA2 phosphorylation and AA release in response to PMA and ATP stimulation in mouse astrocytes are mediated by ERKs and p38 MAPK pathways [10]. In the platelets, cPLA2 phosphorylation was induced by p38 MAPK activation [24]. Here, we found that ApoE4 selectively activated p38 but not ERKs. This is consistent with a previous report of greater p38 activation but not ERKs pathway in ApoE4-TR mice [52], suggesting the increase of phosphorylation of cPLA2 in ApoE4 is regulated by p38 MAPK but not ERKs. Interestingly, p38 inhibitors are in drug development pipelines for AD [53].

Our study has strengths and some limitations. We validated our findings of greater cPLA2 activation in cells, in ApoE-TR animal models and in human brains matched by disease stage and differing by genotype. We identified the signaling pathway involved in cPLA2 activation- (MAPK-p38) and validated this in both animal and human brains. Some of the limitations include not examining the effects of ApoE4 on cPLA2 activation on microglia. It is plausible that ApoE4 enhances microglial activation through a cPLA2 dependent mechanism, with unique downstream activation patterns. In the clinical cohort, we did not study cPLA2 expression in *APOE4* homozygote patients without cognitive impairment, as this condition is extremely rare. We also acknowledge that the small sample sizes for both humans and mice studies preclude the full examination of the effect of sex on the association between *APOE4* and neuroinflammation. Future studies will include larger samples sizes and more specific approaches (such as single cell sequencing) to capture cPLA2's activation fingerprint on distinct brain cells.

Conclusions

Overall, using multiple approaches, our study has identified that the activation of cPLA2 is implicated in neuroinflammation and oxidative stress associated with *APOE4* (Fig. 9). Our findings support that induction of the MAPK-p38 pathway as the driving factor for the activation of cPLA2-LTB4 signaling cascade, and our cellular studies prioritize astrocytes as the target cell type. Small molecular inhibitors of

cPLA2 can be tested *in vivo* for their capacity to reduce the risk of AD dementia associated with carrying the *APOE4* allele.

Materials And Methods

Clinical Samples

The frozen hippocampus of AD patients with *APOE4/E4* carriers (N = 9) and no-cognitive impairment (NCI) with *APOE3/E3* carriers (N = 7) were collected from the University of Southern California (USC) Alzheimer Disease Research Center (ADRC) Neuropathology core, which was approved by USC's Institutional Review Board (IRB) protocol (HS-16-00888). The frozen inferior frontal lobe (Brodmann area 10) of the individuals with NCI and the *APOE3/E3* carriers (N = 12) and *APOE3/E4* carriers (N = 10), and persons with AD patients and the *APOE3/E3* (N = 12) and *APOE3/E4* genotypes (N = 10) were obtained from the Rush Alzheimer's Disease Center (RADC) at the Rush University Medical Center. Rush Memory and Aging Project was approved by an Institutional Review Board (IRB) of Rush University Medical Center.

Animals

ApoE3-TR and ApoE4-TR mice were a generous gift from Dr. Patrick Sullivan, in which the endogenous mouse ApoE was replaced by either human APOE3 or APOE4, were created by gene targeting as described previously [54]. All experiments were performed on age-matched male animals (8 months of age) and were approved by the USC Animal Care Committee. Every effort was made to reduce animal stress and to minimize animal usage. The mice were anesthetized with isoflurane and perfused with PBS. The brains were split in half for further analysis.

Cell cultures

Primary astrocytes were obtained from C57JB6, ApoE3-TR and ApoE4-TR mice pups, and cultured as described previously[55]. Briefly, cerebral cortices from each 1 to 3 day-old neonatal mouse were dissected in ice-cold Hanks' Balanced Salt Solution (HBSS) (Corning, 21-021-CV), and digested with 0.25% trypsin for 20 min at 37°C. Trypsinization was stopped by addition of 2-fold volume of DMEM (Corning, 10−013) with 10% fetal bovine serum (FBS) (Omega Scientific, FB-12) and 1% antibiotic-antimycotic (Anti-anti) (Thermo Fisher, 15240062). The cells were dispersed into a single-cell level by repeated pipetting and filtered through 100µ m cell strainers (VWR, 10199-658). After filtering, cells were centrifuged for 5 min at 1000 rpm and resuspended in culture medium supplemented with 10% FBS and antibiotics. Then, cells were seeded in a 75 cm^2 flask and cultured at 37°C in 5% CO2. The medium was changed on the next day and then replaced every 3 days. These mixed glia cultures reached confluence after 7−10 days. Then, the cells were shaken at 250 rpm for 16 h at 37°C to remove microglia and oligodendrocyte progenitor cells. The remaining cells were harvested by digestion with trypsin. At this stage the culture contains 95% astrocytes and was used for further experiments.

Immortalized mouse astrocytes derived from human ApoE3 and ApoE4 knock-in mice [56] were gifts from Dr. David Holtzman and grown in DMEM/F12 (Corning, MT10090CV) containing 10% FBS, 1 mM sodium pyruvate (Thermo Fisher, 11360070), 1 mM geneticin (Thermo Fisher, 10131-035) and 1% anti-anti.

Cell lysate and brain homogenate preparation

The immortalized or primary astrocyte were lysed with 1x RIPA buffer (Cell Signaling Technology, CST 9806) containing protease inhibitor cocktail (Sigma, P8340) and phosphatase inhibitor cocktail (Sigma, P0044), followed by centrifugation at 14,000 gs for 10 min at 4 °C. The supernatant was collected for further analysis.

The mouse cerebral cortex, human hippocampus and inferior frontal cortex were weighed, then RIPA buffer containing protease inhibitor cocktail and phosphatase inhibitor cocktail was added as 1:30 (w/v). Then, the tissue was homogenized using a 2 mL glass dounce tissue grinder, followed by centrifugation with 14,000 gs for 10 min at 4 °C. The supernatant was collected, and the concentration was measured by BCA kit.

cPLA2 protein enrichment

To detect the phosphorylated cPLA2 in mouse cortex homogenates, cPLA2 protein was enriched by immunoprecipitation. For each mouse sample, 5 µg of cPLA2 antibody (Santa Cruz Biotechnology, sc-376618) was conjugated to 50 µL Dynabeads Protein G (Thermo Scientific, 10003D) for 1 hr at room temperature, then 500 µg total protein in 500 µL RIPA was added to the cPLA2-beads complex and incubated with rotation overnight at 4 °C. The beads were washed with 0.1% PBST 3 times by rotation for 5 min. After washing, 30 µL of 1x sample buffer (Bio-Rad, 1610747) was added to the beads and heated for 10 minutes at 100 °C. The supernatant was collected by magnetic force and used for the further Western-blot assay.

Western-blot

The cell lysates, cortex homogenate and enriched cPLA2 proteins were separated by 4–15% mini-precast protein gels (Bio-Rad, 4561086) under reducing conditions and then transferred onto nitrocellulose membranes (Bio-Rad, 1704270). After transferring, membranes were blocked with 5% fat-free milk (Bio-Rad, 1706404) in TBST for 1 h at room temperature, followed by overnight incubation with primary antibody in 5% BSA at 4 °C. Then, the membranes were incubated with HRP conjugated secondary antibody for 1 h at room temperature. Chemiluminescent HRP substrate (Millipore, WBKLS0500) was used for detection. Fujifilm LAS-4000 imager system was used to capture images and the densitometric quantification was done by Gel Quant NET software.

The following antibodies and dilution factors were used: cPLA2 antibody (Santa Cruz Biotechnology, sc-376618) (1:200), phospho-cPLA2 (Ser505) antibody (CST, 53044) (1:1000), phospho-ERK1/2 antibody (CST, 4370) (1:1000), ERK1/2 antibody (CST, 4595) (1:1000), p38 antibody (CST, 9212) (1:1000), phospho-p38 antibody (CST, 4511) (1:1000), GFAP antibody (CST, 12389) (1:1000), Iba-1 antibody

(GeneTex, GTX100042) (1:1000), iNOS antibody (CST, 13120) (1:1000), β-actin antibody (CST, 3700) (1:1000), β-tubulin antibody (CST, 2146) (1:1000), HRP-linked anti-mouse IgG (CST, 7076) (1:2000), HRP-linked anti-rabbit IgG (CST, 7074) (1:2000).

qPCR

The cells and brain specimens were harvested, and RNA was extracted using an RNA extraction kit (Thermo Fisher, K0731). Synthesis of cDNA was done using High-Capacity cDNA Reverse Transcription Kit (Thermo Fisher, 4368814). qPCR was performed using the PowerUp SYBR Green Master Mix (Thermo Fisher, A25742). The following primers were synthesized by Integrated DNA Technologies. The cPLA2 sense (5'-CTGCAAGGCCGAGTGACA-3') and antisense (5'-TTCGCCCACTTCTCTGCAA-3'); mouse Tnfα sense (5'-GCCTCTTCTCATTCCTGCTTG-3') and antisense (5'-CTGATGAGAGGGAGGCCATT-3'); mouse Il1β sense (5'-GCAACTGTTCCTGAACTCAACT-3') and antisense (5'-ATCTTTTGGGGTCCGTCAACT-3'); mouse Il6 sense (5'-TAGTCCTTCCTACCCCAATTTCC-3') and antisense (5'-TTGGTCCTTAGCCACTCCTTC-3'); mouse Ccl2 sense (5'-GTCCCTGTCATGCTTCTGG-3') and antisense (5'-GCTCTCCAGCCTACTCATTG-3'); mouse Mip1α sense (5'- TGAAACCAGCAGCCTTTGCTC-3') and antisense (5'-AGGCATTCAGTTCCAGGTCAGTG-3'); mouse Mip2 sense (5'-ATCCAGAGCTTGAGTGTGACGC-3') and antisense (5'- AAGGCAAACTTTTTGACCGCC-3'); mouse β-actin sense (5'-ACCTTCTACAATGAGCTGCG-3') and antisense (5'-CTGGATGGCTACGTACATGG-3'); human TNFα sense (5'-ACTTTGGAGTGATCGGCC-3') and antisense (5'-GCTTGAGGGTTTGCTACAAC-3'); human IL1β sense (5'-ATGCACCTGTACGATCACTG-3') and antisense (5'-ACAAAGGACATGGAGAACACC-3');

human IL6 sense (5'-CCACTCACCTCTTCAGAACG-3') and antisense (5'-CATCTTTGGAAGGTTCAGGTTG-3'); human CCL2 sense (5'- TGTCCCAAAGAAGCTGTGATC-3') and antisense (5'-ATTCTTGGGTTGTGGAGTGAG-3'); human GAPDH sense (5'-ACATCGCTCAGACACCATG-3') and antisense (5'-TGTAGTTGAGGTCAATGAAGGG-3')

AA and DHA efflux assays

To investigate arachidonic acid (AA) and docosahexaenoic acid (DHA) release by cPLA2 and iPLA2 activation respectively, we performed an AA and DHA efflux assay as described previously [2]. ApoE3 and ApoE4 primary astrocytes were seeded at 5000 cells/well in 96-well plates. After 24 h the culture medium was changed with serum-free DMEM containing fatty acid-free BSA (5 mg/mL) (Sigma, A9647) and 3H-AA (1 μCi/mL) or 14C-DHA (1 μCi/mL) (Moravek) for 24 h. Then, the cells were washed twice with 100 μL of DMEM and 100 μL of DMEM containing BSA (5 mg/mL) was added. After 30 minutes, the medium was removed and 100 μL of ATP (100 μM) in DMEM without BSA was added. After 15 minutes, cell culture medium was collected and transferred to scintillation vials filled with 3 mL of scintillation cocktail. The cells were solubilized in 90 μL of NaOH (0.5N) for 5 minutes and neutralized with 60 μL PBS, and then transferred to scintillation vials filled with 3 mL of scintillation cocktail. After mixing rigorously, the vials were counted in a Beckman LS6500 liquid scintillation counter (Beckman Coulter). The efflux of AA and DHA were assessed by the ratio of cholesterol in the medium to total cholesterol (medium and cell lysate). The change of AA and DHA efflux was calculated by subtracting the levels of

AA and DHA in the ATP treated group to ATP non-treated group for each genotype. WT primary astrocytes were plated and labelled with ^{3}H-AA (1 µCi/mL) or ^{14}C-DHA (1 µCi/mL) as described above. Then, the cells were washed twice with 100 µL of DMEM. After wash, 10 µL of DMEM containing BSA and 0.2 µM recombinant ApoE3 or ApoE4 protein were added. After 24 h, the medium was removed and 100 µL of ATP (100 µM) in DMEM without BSA was added. The AA and DHA efflux were measured as described above after 15 minutes.

cPLA2 activity assay

cPLA2 activity was detected by cPLA2 activity assay kit (Cayman Chemical, 765021). The mouse cortex was homogenized into HEPES buffer (50 mM, pH 7.4, containing 1 mM EDTA) as 1:10 (w/v) and supernatant was collected after centrifuged and used for cPLA2 activity detection.

LTB4 and PGE2 measurement

For the LTB4 an PGE2 measurement in the human brain samples, brain tissue was weighed, then PBS containing 1 mM EDTA, 10 µM indomethacin (Cox inhibitor, Sigma I8280) and 10 µM NDGA (Lox inhibitor, Sigma 479975) as 1:10 (w/v) were added. Then, the tissue was homogenized using a 2 mL glass dounce tissue grinder, followed by centrifugation with 8,000 xg for 10 minutes at 4 °C. The supernatant was collected, and the concentration was measured by a BCA kit. LTB4 and PGE2 levels were detected by the assay kit (LTB4 ELISA Kit, Cayman Chemical, 10009292; PGE2 ELISA Kit, Cayman Chemical, 500141).

For the LTB4 measurement in the cells, ApoE3 and ApoE4 primary astrocytes were seeded in 24-wells plate with the intensity of 100,000 cells per well. Forty-eight hours later, cells were pre-treated with cPLA2 inhibitor-Pyrrophenone (500 nM, Sigma, 5305380001) in the DMEM culture medium without FBS but containing N2 supplement for 30 minutes, followed by the treatment with vehicle or TNFα (10 ng/mL) (R&D Systems, 210-TA-005) plus IFNγ (100 ng/mL) (Sigma, SRP3058) together for 18 hours. Then, the culture media and cell lysate were collected. LTB4 levels were measured in 4-fold concentrated medium by the assay kit.

ROS measurement

ROS were detected by the DCFDA cellular ROS detection assay kit (Abcam, ab113851). ApoE3 and ApoE4 primary astrocyte were seeded in dark, clear bottom 96-wells plate with the intensity of 20,000 cells per well. Forty-eight hours later, cells were pre-treated with cPLA2 inhibitor (1 µM) in the DMEM culture medium without FBS but containing N2 supplement for 30 minutes, followed by the treatment with vehicle or TNFα (10 ng/mL) plus IFNγ (100 ng/mL) together for 24 hours. After removing the media and washing plate once with 1x assay buffer, the cells were stained with DCFDA solution (100 µL/well) for 45 minutes at 37 °C in the dark. Then, the DCFDA solution was removed and the 1x assay buffer (100 µL/well) was added into the plate. ROS levels were measured using a fluorescent plate reader at Excision/Emission = 485/585 nm.

Statistical analysis

Descriptive results are presented as the mean ± SD. Data were analyzed using Student's unpaired t-test or ANOVA. The cPLA2 phosphorylation was compared in APOE groups using linear regression model, adjusting for age, sex, and Braak stage. Non-parametric tests were used for non-normally distributed data. Statistical significance was present at $p < 0.05$. Statistical program R, version 3.5 was used.

Abbreviations

ApoE, Apolipoprotein E; ApoE-TR, ApoE-targeted replacement; AD, Alzheimer disease; NCI, no cognitive impairment; cPLA2, calcium-dependent cytosolic phospholipase A2; iPLA2, calcium-independent phospholipase A2 (iPLA2); DHA, docosahexaenoic acid; AA, arachidonic acid; LPC, lysophosphatidylcholine; LTB4, leukotriene B4; PGE2, prostaglandin E2; ROS, reactive oxygen species; iNOS, inducible nitric oxide synthase; NO, nitric oxide; COX, cyclooxygenase; LOX, lipoxygenase; MAPK, mitogen-activated protein kinase; MAVS, mitochondrial antiviral-signaling protein; NF-kB; nuclear factor kappa-light-chain-enhancer of activated B cells; LPS, lipopolysaccharide; CRP, C reactive protein.

Declarations

Ethics approval and consent to participate

The frozen hippocampus samples were collected from the University of Southern California (USC) Alzheimer Disease Research Center (ADRC) Neuropathology core, which was approved by USC's Institutional Review Board (IRB) protocol (HS-16-00888). The frozen inferior frontal lobe (Brodmann area 10) were obtained from the Rush Alzheimer's Disease Center (RADC) at the Rush University Medical Center. Rush Memory and Aging Project was approved by an Institutional Review Board (IRB) of Rush University Medical Center.

Consent for publication

Not applicable.

Availability of data and materials

All data used and analyzed for the current study are available from the corresponding author on reasonable request.

Competing interests

The authors declare that they have no competing interests.

Funding

HNY was supported by R21AG056518, R01AG055770, R01AG054434, R01AG067063 from the National Institute on Aging. This work was also supported by P50AG05142 (HCC), P30 AG10161 (DAB), R01 AG17917 (DAB), R01 NS084965 (ZA), and RF1 AG059621 (ZA) from the National Institutes of Health. Contribution of SIR was funded by Intramural Program of National Institute of Alcohol Abuse and Alcoholism. Funders had no role in study design, data collection, data analysis, interpretation, or writing of the report.

Authors' contributions

HNY and SW designed experiments. SW and BL performed experiments. SW wrote manuscript. PMS supplied mice. DAB and ZA supplied human cortex samples. HCC and CM supplied human hippocampus samples. VS, AF, SIR, DAB, ZA, HC, CM, and HNY revised manuscript.

Acknowledgements

We thank Dr. Caleb Finch for critically reviewing the manuscript. We thank Dr. David M. Holtzman for providing us with ApoE3 and ApoE4 immortalized astrocytes.

References

1. Six DA, Dennis EA. The expanding superfamily of phospholipase A2 enzymes: classification and characterization. Biochimica et Biophysica Acta (BBA)-Molecular Cell Biology of Lipids. 2000;1488:1–19.

2. Strokin M, Sergeeva M, Reiser G. Docosahexaenoic acid and arachidonic acid release in rat brain astrocytes is mediated by two separate isoforms of phospholipase A2 and is differently regulated by cyclic AMP and Ca2+. Br J Pharmacol. 2003;139:1014–22.

3. Cheon Y, Kim H-W, Igarashi M, Modi HR, Chang L, Ma K, Greenstein D, Wohltmann M, Turk J, Rapoport SI. Disturbed brain phospholipid and docosahexaenoic acid metabolism in calcium-independent phospholipase A2-VIA (iPLA2β)-knockout mice. Biochimica et Biophysica Acta (BBA)-Molecular Cell Biology of Lipids. 2012;1821:1278–86.

4. Gijón MA, Leslie CC. Regulation of arachidonic acid release and cytosolic phospholipase A2 activation. J Leukoc Biol. 1999;65:330–6.

5. Berk P, Stump D: **Mechanisms of cellular uptake of long chain free fatty acids**. In *Lipid Binding Proteins within Molecular and Cellular Biochemistry*. Springer; 1999: 17–31.

6. Leslie CC. Cytosolic phospholipase A2: physiological function and role in disease. Journal of lipid research. 2015;56:1386–402.

7. Chao CC, Gutierrez-Vazquez C, Rothhammer V, Mayo L, Wheeler MA, Tjon EC, Zandee SEJ, Blain M, de Lima KA, Takenaka MC, et al. Metabolic Control of Astrocyte Pathogenic Activity via cPLA2-MAVS. Cell. 2019;179:1483–98 e1422.

8. Chuang DY, Simonyi A, Kotzbauer PT, Gu Z, Sun GY. Cytosolic phospholipase A 2 plays a crucial role in ROS/NO signaling during microglial activation through the lipoxygenase pathway. J Neuroinflamm. 2015;12:199.

9. Lin L-L, Wartmann M, Lin AY, Knopf JL, Seth A, Davis RJ. cPLA2 is phosphorylated and activated by MAP kinase. Cell. 1993;72:269–78.

10. Xu J, Weng Y-I, Simonyi A, Krugh BW, Liao Z, Weisman GA, Sun GY. Role of PKC and MAPK in cytosolic PLA2 phosphorylation and arachadonic acid release in primary murine astrocytes. J Neurochem. 2002;83:259–70.

11. Perez-Nievas BG, Stein TD, Tai H-C, Dols-Icardo O, Scotton TC, Barroeta-Espar I, Fernandez-Carballo L, De Munain EL, Perez J, Marquie M. Dissecting phenotypic traits linked to human resilience to Alzheimer's pathology. Brain. 2013;136:2510–26.

12. Stephenson DT, Lemere CA, Selkoe DJ, Clemens JA. Cytosolic phospholipase A2 (cPLA2) immunoreactivity is elevated in Alzheimer's disease brain. Neurobiol Dis. 1996;3:51–63.

13. Colangelo V, Schurr J, Ball MJ, Pelaez RP, Bazan NG, Lukiw WJ. Gene expression profiling of 12633 genes in Alzheimer hippocampal CA1: transcription and neurotrophic factor down-regulation and up-regulation of apoptotic and pro-inflammatory signaling. J Neurosci Res. 2002;70:462–73.

14. Sanchez-Mejia RO, Newman JW, Toh S, Yu GQ, Zhou Y, Halabisky B, Cisse M, Scearce-Levie K, Cheng IH, Gan L, et al. Phospholipase A2 reduction ameliorates cognitive deficits in a mouse model of Alzheimer's disease. Nat Neurosci. 2008;11:1311–8.

15. Sun GY, He Y, Chuang DY, Lee JC, Gu Z, Simonyi A, Sun AY. Integrating cytosolic phospholipase A 2 with oxidative/nitrosative signaling pathways in neurons: a novel therapeutic strategy for AD. Mol Neurobiol. 2012;46:85–95.

16. Palavicini JP, Wang C, Chen L, Hosang K, Wang J, Tomiyama T, Mori H, Han X. Oligomeric amyloid-beta induces MAPK-mediated activation of brain cytosolic and calcium-independent phospholipase A 2 in a spatial-specific manner. Acta neuropathologica communications. 2017;5:56.

17. Sundaram JR, Chan ES, Poore CP, Pareek TK, Cheong WF, Shui G, Tang N, Low C-M, Wenk MR, Kesavapany S. Cdk5/p25-induced cytosolic PLA2-mediated lysophosphatidylcholine production regulates neuroinflammation and triggers neurodegeneration. J Neurosci. 2012;32:1020–34.

18. Qu B, Gong Y, Gill JM, Kenney K, Diaz-Arrastia R. Heterozygous knockout of cytosolic phospholipase A2α attenuates Alzheimer's disease pathology in APP/PS1 transgenic mice. Brain research. 2017;1670:248–52.

19. Tao Q, Ang TFA, DeCarli C, Auerbach SH, Devine S, Stein TD, Zhang X, Massaro J, Au R, Qiu WQ. Association of Chronic Low-grade Inflammation With Risk of Alzheimer Disease in ApoE4 Carriers. JAMA Netw Open. 2018;1:e183597.

20. Ramassamy C, Averill D, Beffert U, Theroux L, Lussier-Cacan S, Cohn JS, Christen Y, Schoofs A, Davignon J, Poirier J. Oxidative insults are associated with apolipoprotein E genotype in Alzheimer's disease brain. Neurobiol Dis. 2000;7:23–37.

21. Tomaszewski N, He X, Solomon V, Lee M, Mack WJ, Quinn JF, Braskie MN, Yassine HN. Effect of APOE Genotype on Plasma Docosahexaenoic Acid (DHA), Eicosapentaenoic Acid, Arachidonic Acid, and Hippocampal Volume in the Alzheimer's Disease Cooperative Study-Sponsored DHA Clinical Trial. J Alzheimers Dis. 2020;74:975–90.

22. Yassine HNRV, Mack WJ, Quinn JF, Yurko-Mauro K, Bailey-Hall E, Aisen PS, Chui HC, Schneider LS. The effect of APOE genotype on the delivery of DHA to cerebrospinal fluid in Alzheimer's disease. Alzheimer's Reaserch Therapy. 2016;8:25.

23. Moore SA. Polyunsaturated fatty acid synthesis and release by brain-derived cells in vitro. J Mol Neurosci. 2001;16:195–200.

24. Kramer RM, Roberts EF, Um SL, Borsch-Haubold AG, Watson SP, Fisher MJ, Jakubowski JA. p38 mitogen-activated protein kinase phosphorylates cytosolic phospholipase A2 (cPLA2) in thrombin-stimulated platelets. Evidence that proline-directed phosphorylation is not required for mobilization of arachidonic acid by cPLA2. J Biol Chem. 1996;271:27723–9.

25. Yun B, Lee H, Jayaraja S, Suram S, Murphy RC, Leslie CC. Prostaglandins from Cytosolic Phospholipase A2α/Cyclooxygenase-1 Pathway and Mitogen-activated Protein Kinases Regulate Gene Expression in Candida albicans-infected Macrophages. J Biol Chem. 2016;291:7070–86.

26. Vitek MP, Brown CM, Colton CA. APOE genotype-specific differences in the innate immune response. Neurobiol Aging. 2009;30:1350–60.

27. Colton CA, Brown CM, Cook D, Needham LK, Xu Q, Czapiga M, Saunders AM, Schmechel DE, Rasheed K, Vitek MP. APOE and the regulation of microglial nitric oxide production: a link between genetic risk and oxidative stress. Neurobiol Aging. 2002;23:777–85.

28. Guo L, LaDu MJ, Van Eldik LJ. A dual role for apolipoprotein e in neuroinflammation: anti- and pro-inflammatory activity. J Mol Neurosci. 2004;23:205–12.

29. Chen S, Averett NT, Manelli A, Ladu MJ, May W, Ard MD. Isoform-specific effects of apolipoprotein E on secretion of inflammatory mediators in adult rat microglia. J Alzheimers Dis. 2005;7:25–35.

30. Shi Y, Yamada K, Liddelow SA, Smith ST, Zhao L, Luo W, Tsai RM, Spina S, Grinberg LT, Rojas JC, et al. ApoE4 markedly exacerbates tau-mediated neurodegeneration in a mouse model of tauopathy. Nature. 2017;549:523–7.

31. Tai LM, Balu D, Avila-Munoz E, Abdullah L, Thomas R, Collins N, Valencia-Olvera AC, LaDu MJ. EFAD transgenic mice as a human APOE relevant preclinical model of Alzheimer's disease. Journal of lipid research. 2017;58:1733–55.

32. Zhu Y, Nwabuisi-Heath E, Dumanis SB, Tai LM, Yu C, Rebeck GW, Ladu MJ. APOE genotype alters glial activation and loss of synaptic markers in mice. Glia. 2012;60:559–69.

33. Ophir G, Amariglio N, Jacob-Hirsch J, Elkon R, Rechavi G, Michaelson DM. Apolipoprotein E4 enhances brain inflammation by modulation of the NF-κB signaling cascade. Neurobiol Dis.

2005;20:709–18.

34. Gale SC, Gao L, Mikacenic C, Coyle SM, Rafaels N, Dudenkov TM, Madenspacher JH, Draper DW, Ge W, Aloor JJ. APOε4 is associated with enhanced in vivo innate immune responses in human subjects. Journal of allergy clinical immunology. 2014;134:127–34. e129.

35. Montine KS, Olson SJ, Amarnath V, Whetsell WO Jr, Graham DG, Montine TJ. Immunohistochemical detection of 4-hydroxy-2-nonenal adducts in Alzheimer's disease is associated with inheritance of APOE4. Am J Pathol. 1997;150:437–43.

36. Egensperger R, Kösel S, von Eitzen U, Graeber MB. Microglial activation in Alzheimer disease: association with APOE genotype. Brain Pathol. 1998;8:439–47.

37. Minett T, Classey J, Matthews FE, Fahrenhold M, Taga M, Brayne C, Ince PG, Nicoll JA, Boche D. CFAS M: **Microglial immunophenotype in dementia with Alzheimer's pathology**. J Neuroinflamm. 2016;13:135.

38. Friedberg JS, Aytan N, Cherry JD, Xia W, Standring OJ, Alvarez VE, Nicks R, Svirsky S, Meng G, Jun G. Associations between brain inflammatory profiles and human neuropathology are altered based on apolipoprotein E ε4 genotype. Sci Rep. 2020;10:1–10.

39. Fonteh AN, Chiang J, Cipolla M, Hale J, Diallo F, Chirino A, Arakaki X, Harrington MG. Alterations in cerebrospinal fluid glycerophospholipids and phospholipase A2 activity in Alzheimer's disease. Journal of lipid research. 2013;54:2884–97.

40. Esposito G, Giovacchini G, Liow JS, Bhattacharjee AK, Greenstein D, Schapiro M, Hallett M, Herscovitch P, Eckelman WC, Carson RE, Rapoport SI. Imaging neuroinflammation in Alzheimer's disease with radiolabeled arachidonic acid and PET. Journal of nuclear medicine: official publication Society of Nuclear Medicine. 2008;49:1414–21.

41. Abdullah L, Evans JE, Emmerich T, Crynen G, Shackleton B, Keegan AP, Luis C, Tai L, LaDu MJ, Mullan M. APOE ε4 specific imbalance of arachidonic acid and docosahexaenoic acid in serum phospholipids identifies individuals with preclinical Mild Cognitive Impairment/Alzheimer's Disease. Aging. 2017;9:964.

42. Gentile MT, Reccia M, Sorrentino P, Vitale E, Sorrentino G, Puca A, Colucci-D'Amato L. Role of cytosolic calcium-dependent phospholipase A2 in Alzheimer's disease pathogenesis. Mol Neurobiol. 2012;45:596–604.

43. Bate C, Williams A. Monomeric amyloid-β reduced amyloid-β oligomer-induced synapse damage in neuronal cultures. Neurobiol Dis. 2018;111:48–58.

44. Osborne C, West E, Bate C. The phospholipase A2 pathway controls a synaptic cholesterol ester cycle and synapse damage. J Cell Sci. 2018;131:jcs211789.

45. Desbène C, Malaplate-Armand C, Youssef I, Garcia P, Stenger C, Sauvée M, Fischer N, Rimet D, Koziel V, Escanyé M-C. **Critical role of cPLA2 in Aβ oligomer-induced neurodegeneration and memory deficit**. *Neurobiology of aging* 2012, 33:1123. e1117-1123. e1129.

46. Last V, Williams A, Werling D. Inhibition of cytosolic phospholipase A 2 prevents prion peptide-induced neuronal damage and co-localisation with beta III tubulin. BMC Neurosci. 2012;13:106.

47. Sanchez-Mejia RO. **Phospholipase A2 reduction ameliorates cognitive deficits in a mouse model of Alzheimer's disease**. *Nat Neurosci* 2008, 11.

48. Zhao N, Ren Y, Yamazaki Y, Qiao W, Li F, Felton LM, Mahmoudiandehkordi S, Kueider-Paisley A, Sonoustoun B, Arnold M, et al. Alzheimer's Risk Factors Age, APOE Genotype, and Sex Drive Distinct Molecular Pathways. Neuron. 2020;106:727–42.e726.

49. Soubhye J, van Antwerpen P, Dufrasne F. Targeting Cytosolic Phospholipase A2alpha for Novel Anti-Inflammatory Agents. Curr Med Chem. 2018;25:2418–47.

50. Koundouros N, Karali E, Tripp A, Valle A, Inglese P, Perry NJ, Magee DJ, Virmouni SA, Elder GA, Tyson AL: **Metabolic Fingerprinting Links Oncogenic PIK3CA with Enhanced Arachidonic Acid-Derived Eicosanoids**. *Cell* 2020.

51. Vezzani A, Balosso S, Ravizza T. Neuroinflammatory pathways as treatment targets and biomarkers in epilepsy. Nature Reviews Neurology. 2019;15:459–72.

52. Salomon-Zimri S, Koren A, Angel A, Ben-Zur T, Offen D, Michaelson DM. The Role of MAPK's Signaling in Mediating ApoE4-Driven Pathology In Vivo. Curr Alzheimer Res. 2019;16:281–92.

53. Scheltens P, Prins N, Lammertsma A, Yaqub M, Gouw A, Wink AM, Chu H-M, van Berckel BNM, Alam J. An exploratory clinical study of p38α kinase inhibition in Alzheimer's disease. Ann Clin Transl Neurol. 2018;5:464–73.

54. Sullivan PM, Mezdour H, Aratani Y, Knouff C, Najib J, Reddick RL, Quarfordt SH, Maeda N. Targeted replacement of the mouse apolipoprotein E gene with the common human APOE3 allele enhances diet-induced hypercholesterolemia and atherosclerosis. J Biol Chem. 1997;272:17972–80.

55. Simonovitch S, Schmukler E, Bespalko A, Iram T, Frenkel D, Holtzman DM, Masliah E, Michaelson DM, Pinkas-Kramarski R. Impaired Autophagy in APOE4 Astrocytes. J Alzheimers Dis. 2016;51:915–27.

56. Morikawa M, Fryer JD, Sullivan PM, Christopher EA, Wahrle SE, DeMattos RB, O'Dell MA, Fagan AM, Lashuel HA, Walz T, et al. Production and characterization of astrocyte-derived human apolipoprotein E isoforms from immortalized astrocytes and their interactions with amyloid-beta. Neurobiol Dis. 2005;19:66–76.

Figures
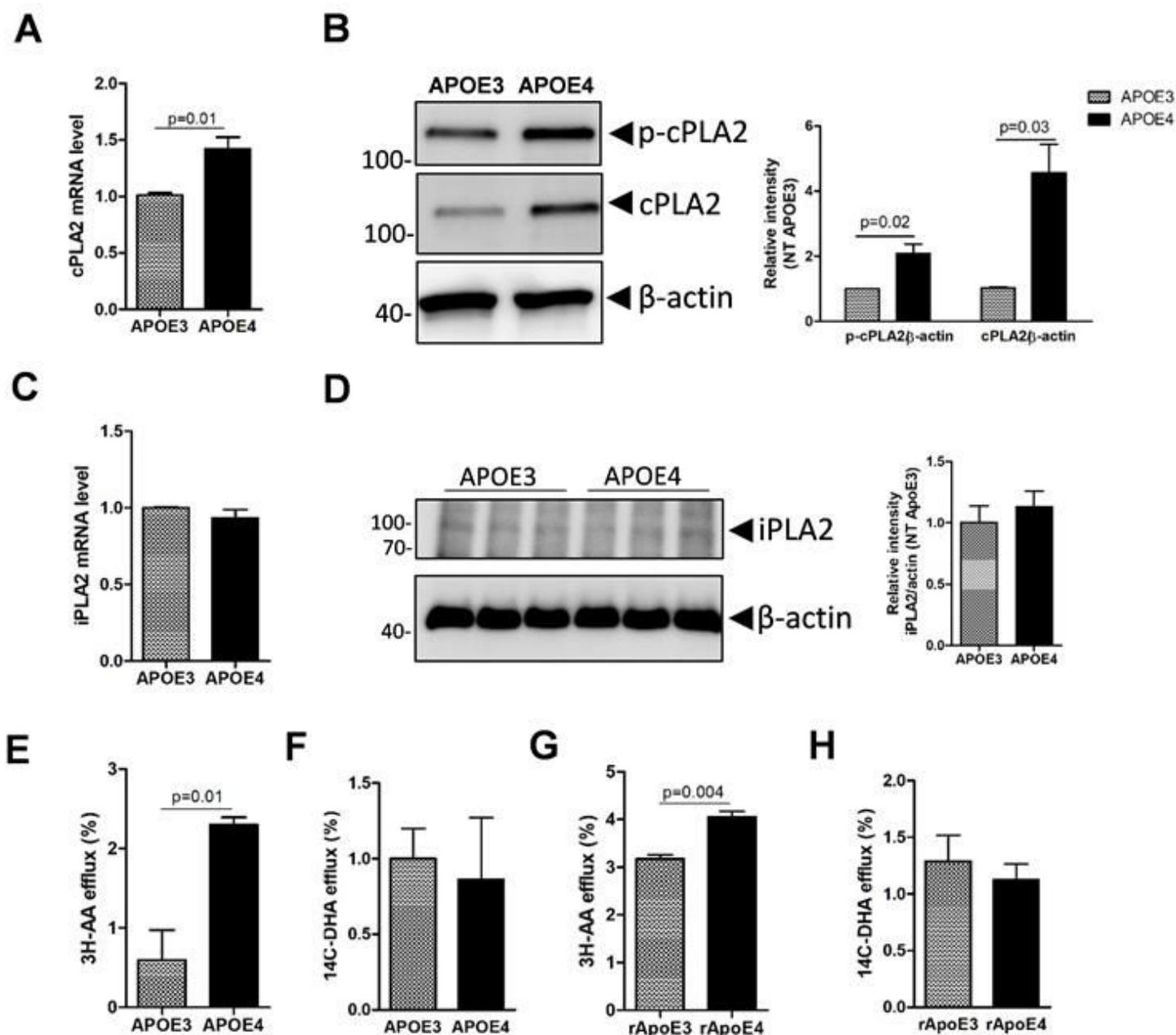
Figure 1

ApoE4 increases cPLA2 but not iPLA2 expression in mouse primary astrocytes. A, cPLA2 mRNA levels in primary astrocytes from APOE3 and APOE4-TR mice. B, cPLA2 and phosphorylated cPLA2 (p-cPLA2) protein levels in primary astrocytes from ApoE3 and ApoE4-TR mice (left) were detected by densitometry (western blot -WB). Quantification of WB from three independent experiments (right). C, iPLA2 mRNA levels in primary astrocytes from ApoE3 and ApoE4-TR mice. D, iPLA2 protein levels in primary astrocyte cultures from ApoE3 and ApoE4-TR mice (left) was detected by WB. Quantification of WB from three independent experiments (right). E, F, Primary astrocytes from ApoE3 and ApoE4-TR mice were incubated with 3H-labelled AA (E) or 14C-labeled DHA (F) for 24h, followed by induction by 100nM ATP for 15min. The efflux of 3H-AA (E) and 14C-DHA (F) from cells to media was measured by scintillation counting. G, H, Primary astrocytes from C57BL/6 wild type mice were labelled with 3H-AA (G) or 14C-DHA (H) for 24h

and then treated with recombinant ApoE3 or ApoE4 for 24h, followed by induction with 100nM ATP for 15min. 3H-AA (G) and 14C-DHA (H) efflux was measured by scintillation counting.
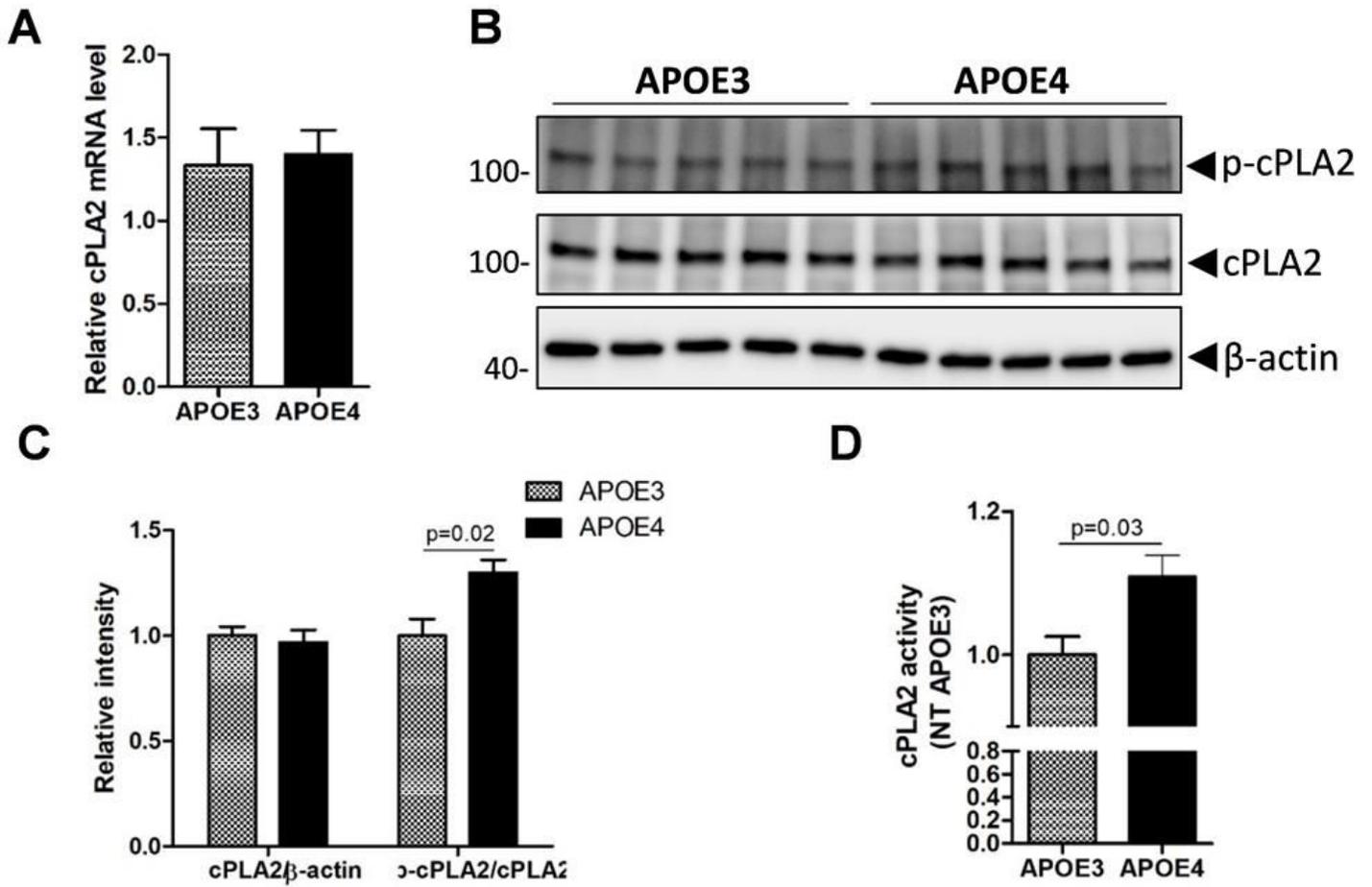
Figure 2

cPLA2 and phosphorylated-cPLA2 level in 8-month old ApoE3-TR and ApoE4-TR mouse brains. The cortex of 8-month old ApoE3 and ApoE4-TR mice were collected. A, cPLA2 mRNA level in the cortex was detected by qPCR. B, phosphorylated-cPLA2 and total cPLA2 protein levels in cortex were detected by densitometry (western-blot). C, Densitometric quantification of blotting shown in B from three independent experiments. D, cPLA2 activity in mouse cortex homogenates were measured by cPLA2 activity assay kit. (n=5 for each genotype, 3 males and 2 females).
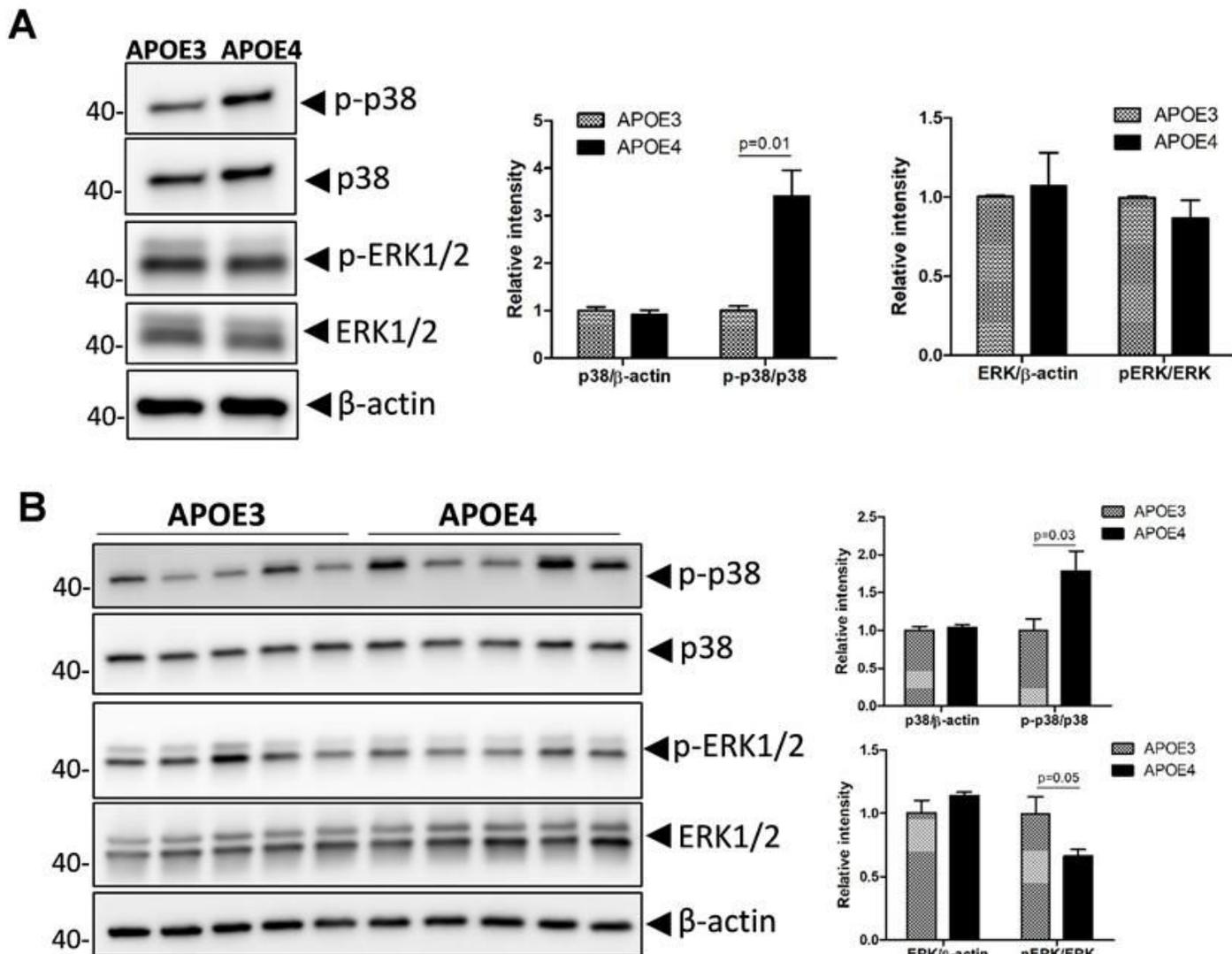
Figure 3

Increased phosphorylated-cPLA2 in APOE4 is mediated by p38 MAPK. A, Phosphorylated and total p38 and ERK levels in primary astrocyte from ApoE3 and ApoE4-TR mice were detected by WB densitometry (left). Quantification of WB from three independent experiments (right). B, Phosphorylated and total p38 and ERK levels in cortical homogenates from APOE3 and APOE4-TR mice were detected by WB (left). Quantification of WB from three independent experiments (right). WB: Western Blot
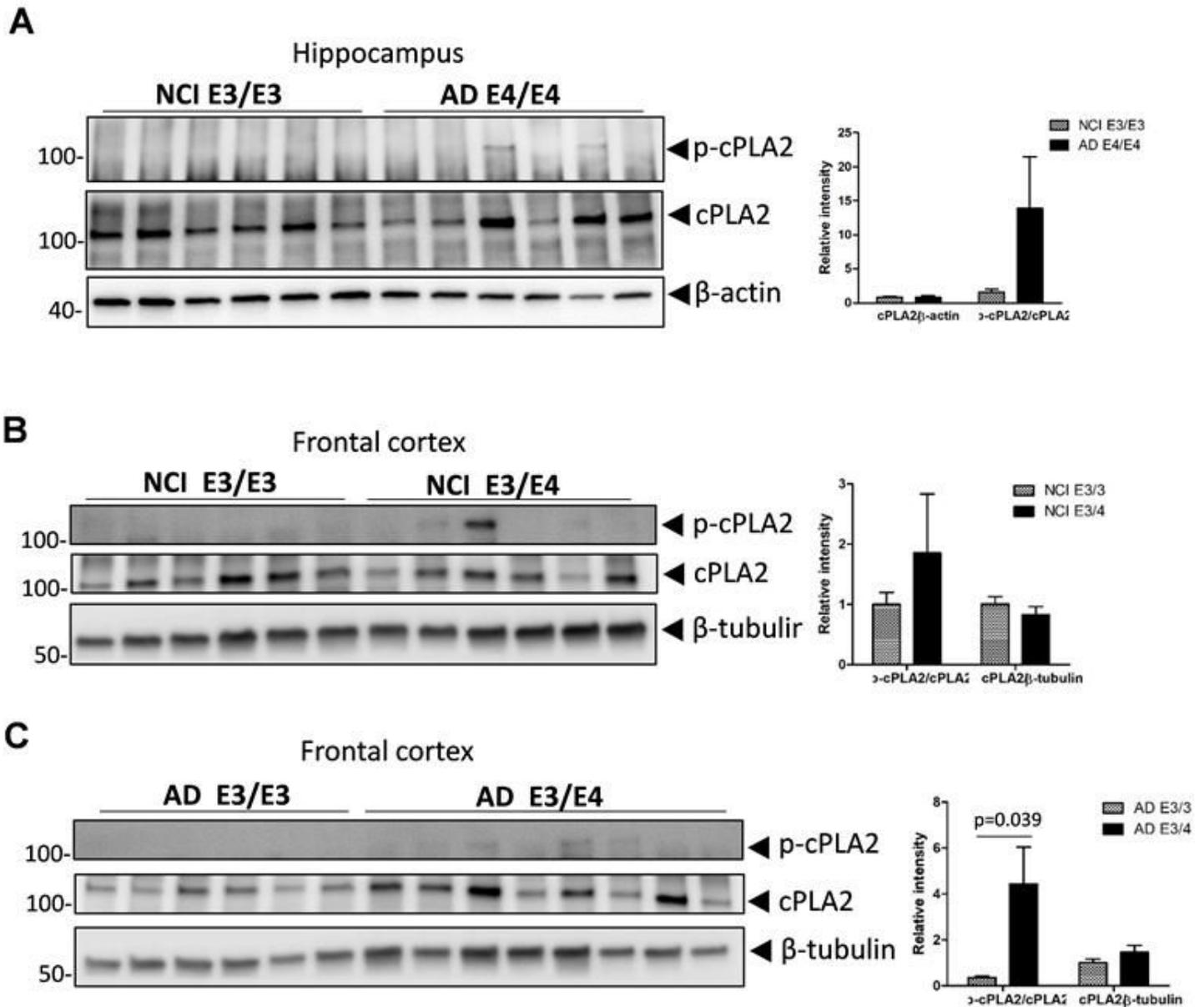
Figure 4

cPLA2 and phosphorylated-cPLA2 levels in the brains of persons with different APOE genotypes. A, p-cPLA2 and cPLA2 protein levels in hippocampus from persons with no cognitive impairment (NCI) carrying E3/E3 and AD patients carrying E4/E4 were detected by WB (left). Quantification of WB from three independent experiments (right). (n=7 (F5/M2) NCI E3/E3; n=9 (F6/M3), AD E4/E4). B, p-cPLA2 and cPLA2 protein levels in inferior frontal cortex from persons with NCI were detected by WB densitometry (left). Quantification of WB from three independent experiments (right). (n=12 (F6/M6), NCI E3/E3; n=10 (F5/M5), NCI E4/E4). C, p-cPLA2 and cPLA2 protein level in inferior frontal cortex from AD patients were detected by WB (left). Quantification of WB from three independent experiments (right). (n=12 (F5/M7), AD E3/E3; n=10 (F6/M4), AD E4/E4). WB: Western Blot
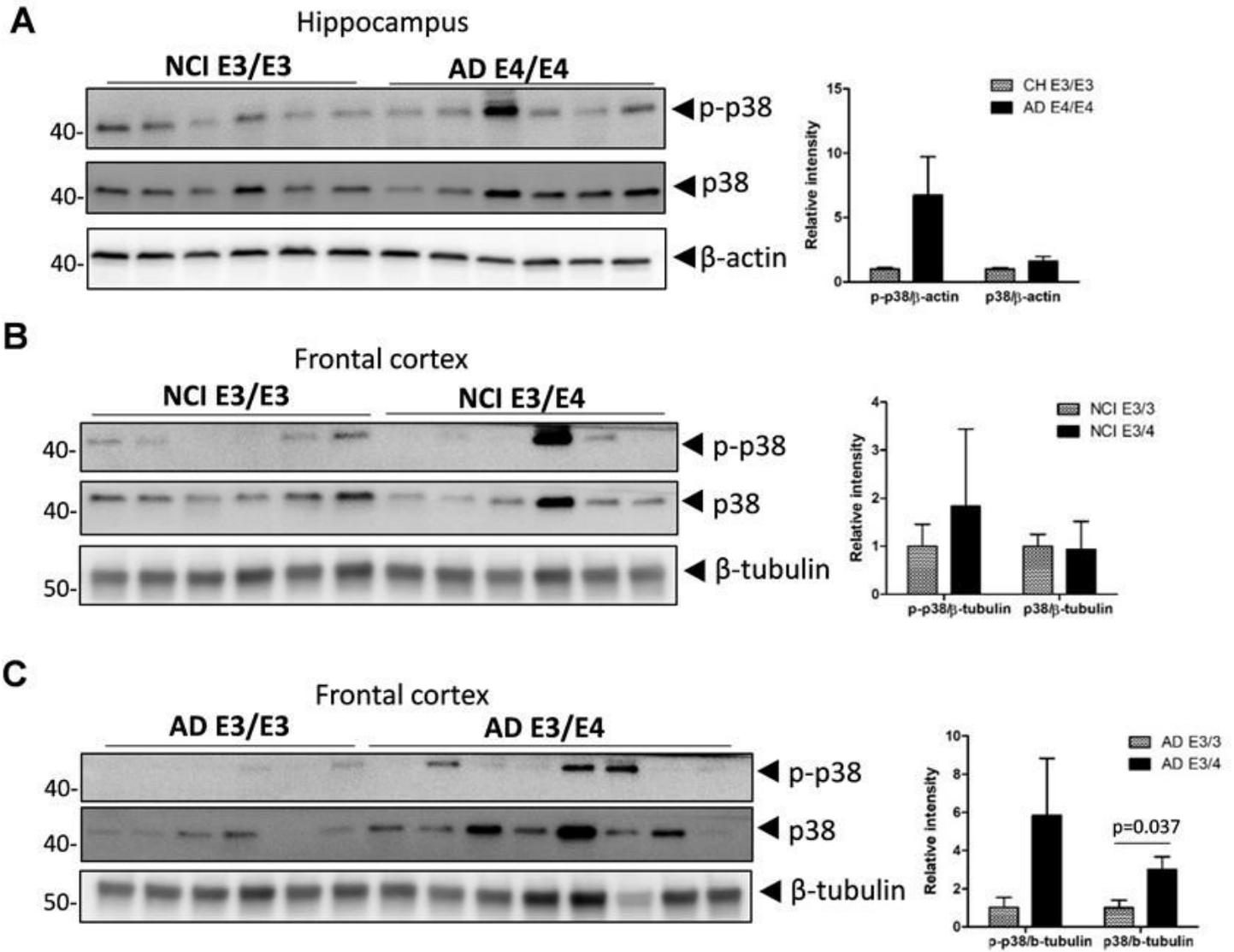
Figure 5

p38 levels in the brains of humans with different APOE genotypes. A, p-p38 and p38 protein levels in hippocampus from persons with no cognitive impairment (NCI) carrying E3/E3 and AD patients carrying E4/E4 were detected by WB (left). Quantification of WB from three independent experiments (right). ((n=7 (F5/M2) for NCI E3/E3; n=9 (F6/M3) for AD E4/ E4). B, p-p38 and p38 protein levels in inferior frontal cortex from persons with NCI were detected by WB densitometry (left). Quantification of WB from three independent experiments (right). (n=12 (F6/M6) for NCI E3/E3; n=10 (F5/M5) for NCI E4/E4). C, p-p38 and p38 protein level in inferior frontal cortex from AD patients were detected by WB (left). Quantification of WB from three independent experiments (right). (n=12 (F5/M7) for AD E3/E3; n=10 (F6/M4) for AD E4/E4). WB: Western blot
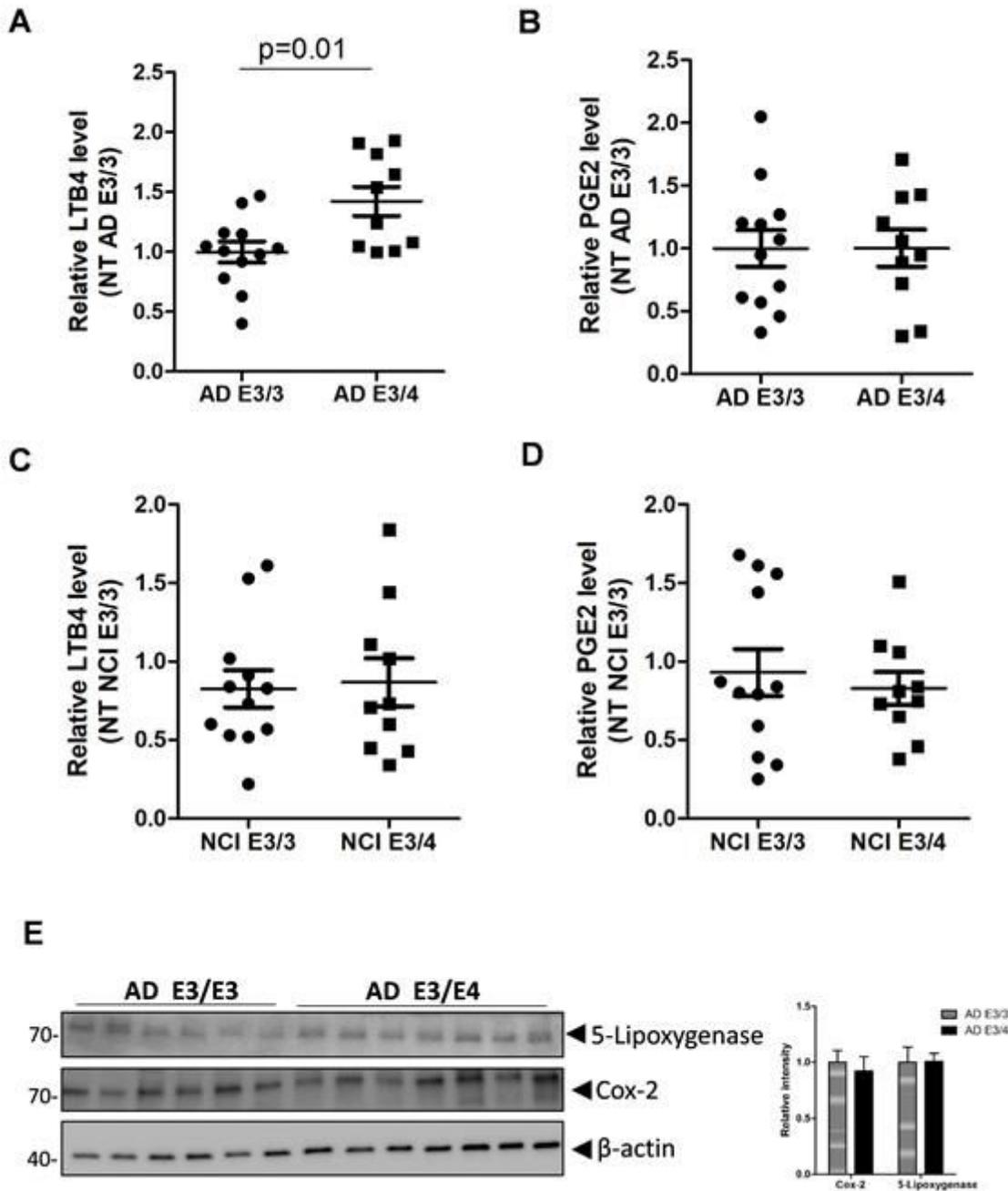
Figure 6

LTB4 and PGE2 levels in cortex of human with different APOE genotypes. LTB4 (A, C) and PGE2 (B, D) levels in the inferior frontal cortex of AD patients (A, B) and NCI participants (C, D) with different APOE genotypes. E, 5-Lipoxygenase and cyclooxygenase 2 protein levels in inferior frontal cortex from AD patients were detected by WB (left). Quantification of WB from three independent experiments (right). (n=12 (F6/M6) for NCI E3/E3; n=10 (F5/M5) for NCI E4/E4; n=12 (F5/M7) for AD E3/E3; n=10 (F6/M4) for AD E4/E4).
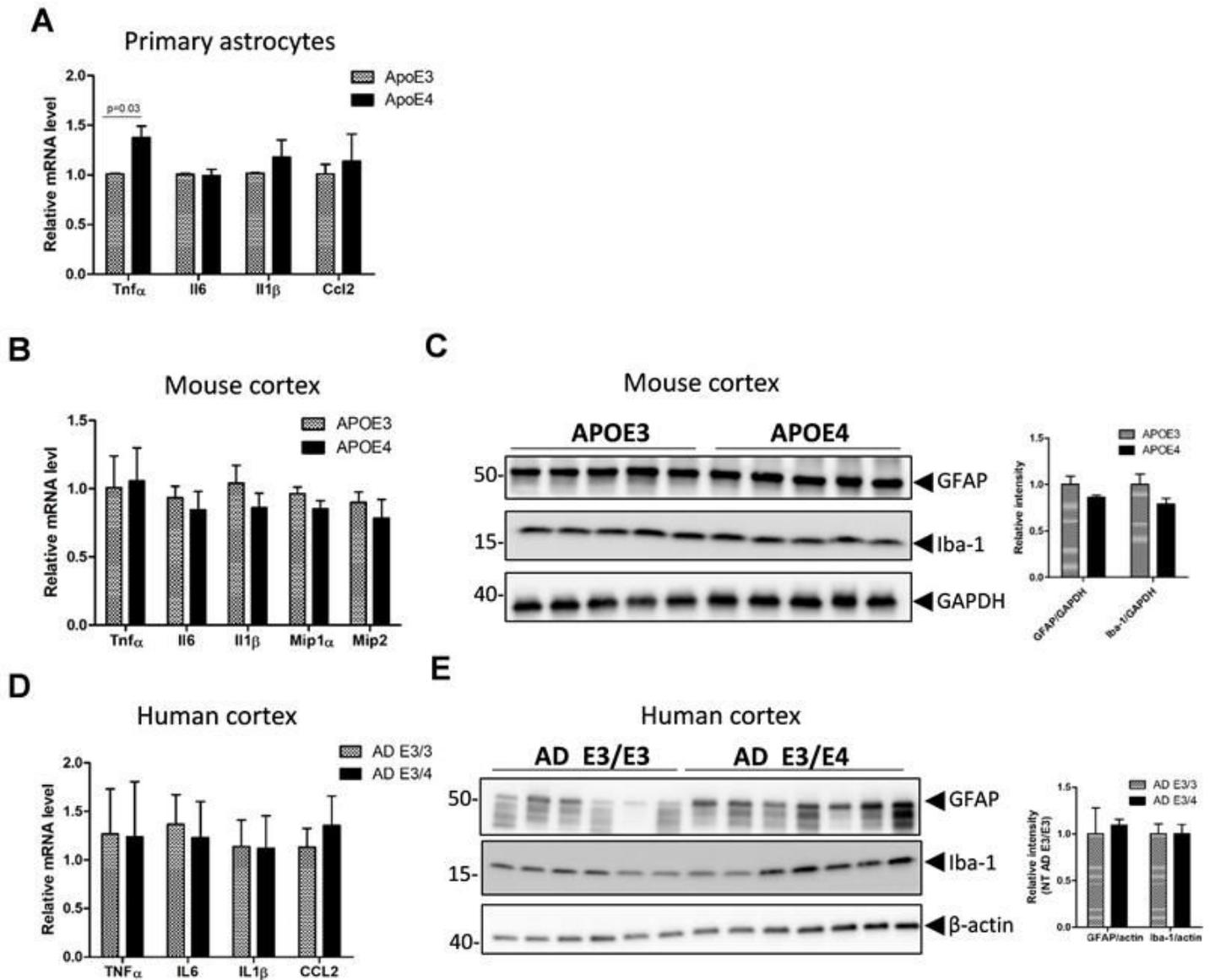
Figure 7

Inflammatory responses in primary astrocytes, mouse and human cortex with different APOE genotypes. A, mRNA levels of pro-inflammatory markers in the primary astrocyte from ApoE3-TR or ApoE4-TR mice. B, mRNA levels of pro-inflammatory cytokines in the cortex of ApoE3-TR or ApoE4-TR mice. C, GFAP and Iba-1 expression in the cortex of ApoE3-TR or ApoE4-TR mice. (n=5, 3 males and 2 females for B and C). D, mRNA levels of pro-inflammatory markers in inferior frontal cortex from AD patients. E, GFAP and Iba-1 expression in inferior frontal cortex AD patients. (n=12 (F5/M7) for AD E3/E3; n=10 (F6/M4) for AD E4/E4).
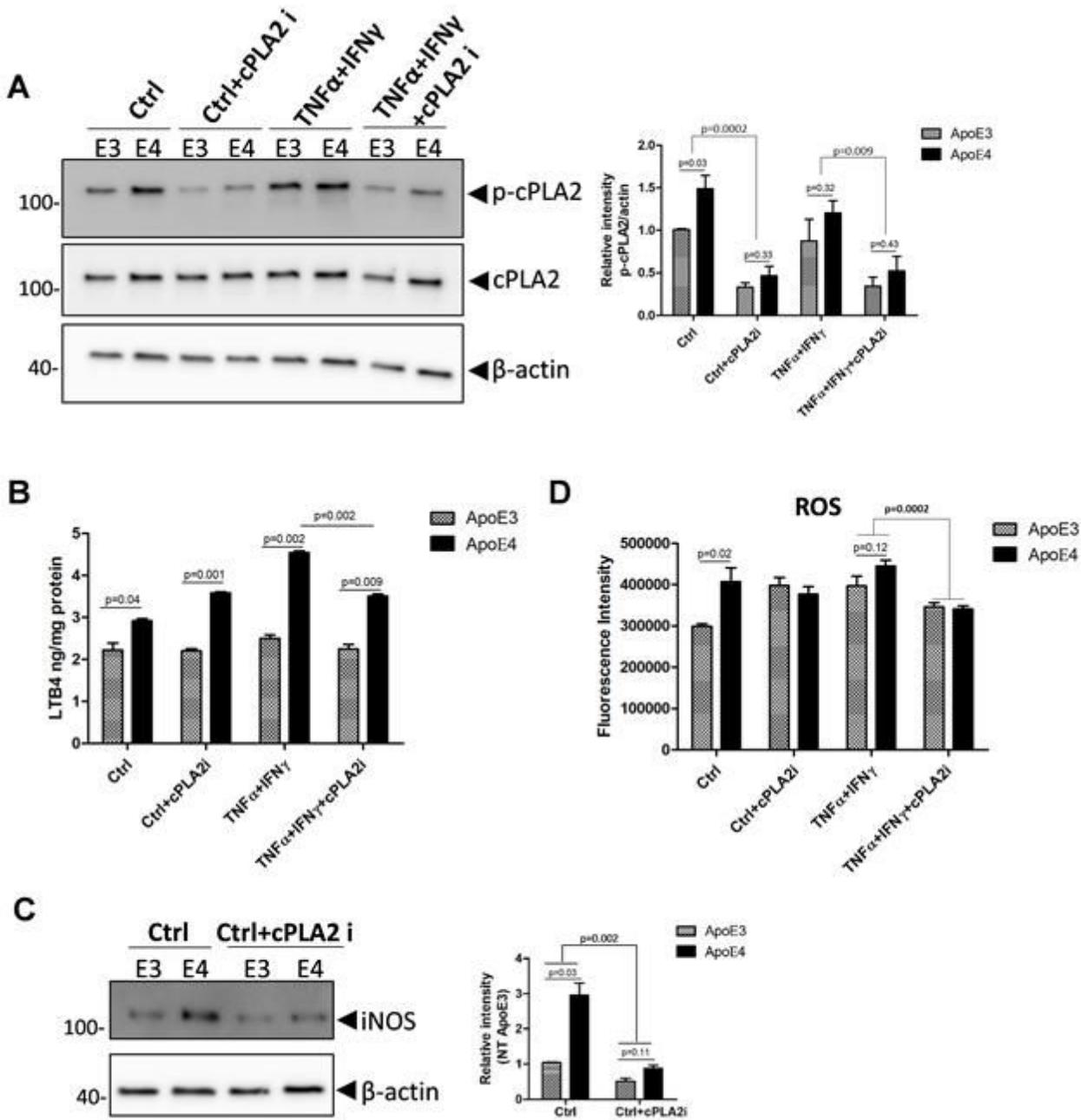
Figure 8

Inhibition of cPLA2 reduces ApoE4 mediated up-regulation of LTB4, ROS and iNOS levels. (A-C) ApoE3 and ApoE4 primary astrocyte from mouse were pre-treated with cPLA2 inhibitor- pyrrophenone (500nM) for 30 min and then treated with medium or TNFα plus IFNγ together for 18 hours. Total and phosphorylated-cPLA2 were detected by WB (left). Quantification of WB from three independent experiments (right) (A). LTB4 levels in the culture medium were measured by the assay kit (B). iNOS expression was detected by WB (left). Quantification of WB from three independent experiments (right) (C). D, ApoE3 and ApoE4 primary astrocyte were pre-treated with cPLA2 inhibitor-pyrrophenone (1μM) for 30 min and then treated with medium or TNFα plus IFNγ together for 24h. The ROS level were detected by DCFDA probe. Two-way ANOVA was used in A, C and D for group comparisons.
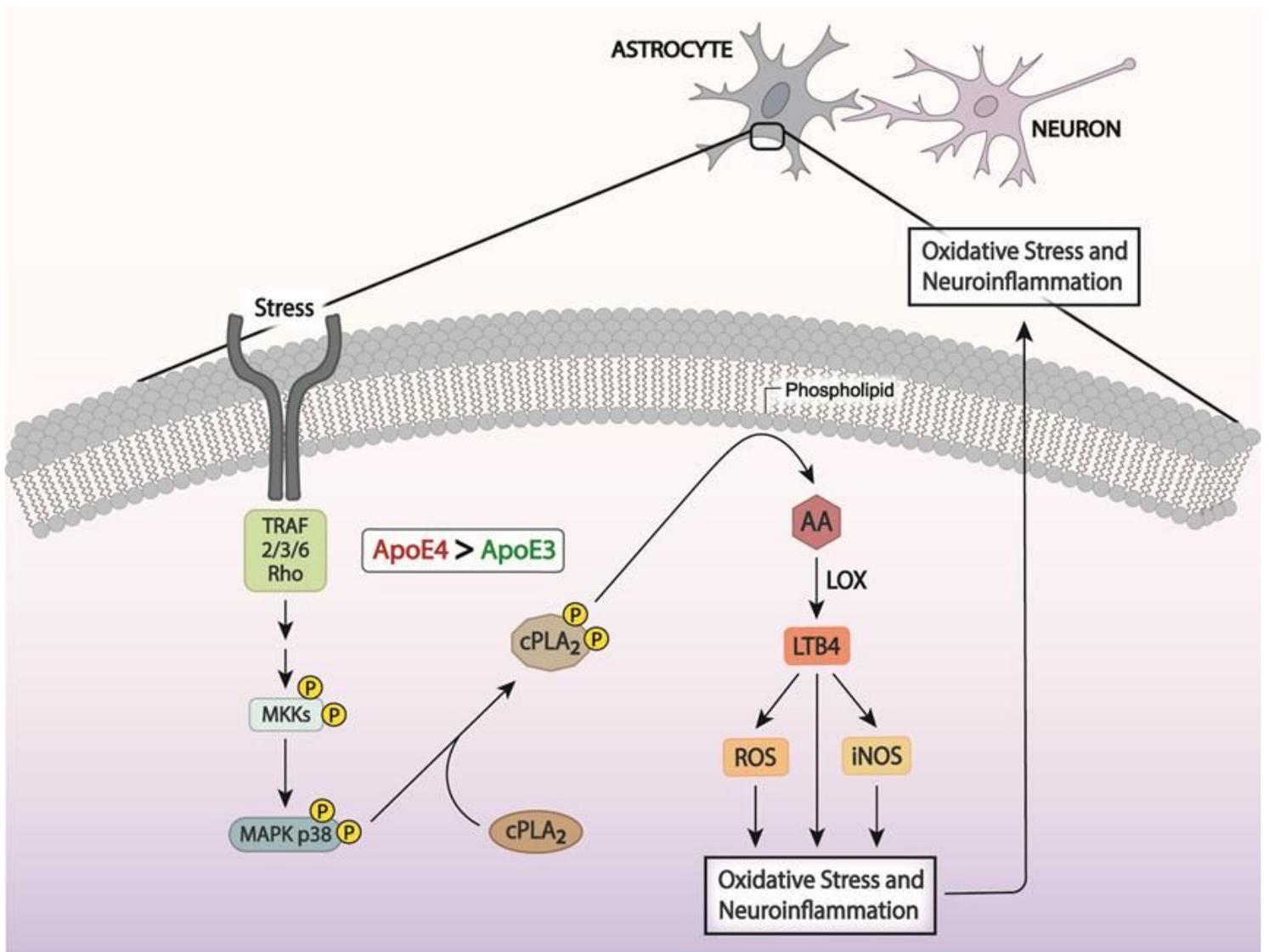
Figure 9

Illustration of ApoE4 in astrocytes inducing greater cPLA2 activation than ApoE3 through the p38 MAPK pathway, leading to more LTB4, iNOS and ROS production, increased oxidative stress and neuroinflammation.